Structure–function analysis of varicella-zoster virus glycoprotein H identifies domain-specific roles for fusion and skin tropism

Susan E. Vleck[a,b,1,2], Stefan L. Oliver[a,b,1], Jennifer J. Brady[b], Helen M. Blau[b], Jaya Rajamani[a,b], Marvin H. Sommer[a,b], and Ann M. Arvin[a,b]

Departments of [a]Pediatrics and [b]Microbiology and Immunology, Stanford University School of Medicine, Stanford, CA 94305

Edited by Bernard Roizman, University of Chicago, Chicago, IL, and approved September 30, 2011 (received for review July 17, 2011)

Enveloped viruses require membrane fusion for cell entry and replication. For herpesviruses, this event is governed by the multiprotein core complex of conserved glycoproteins (g)B and gH/gL. The recent crystal structures of gH/gL from herpes simplex virus 2, pseudorabies virus, and Epstein–Barr virus revealed distinct domains that, surprisingly, do not resemble known viral fusogens. Varicella-zoster virus (VZV) causes chicken pox and shingles. VZV is an α-herpesvirus closely related to herpes simplex virus 2, enabling prediction of the VZV gH structure by homology modeling. We have defined specific roles for each gH domain in VZV replication and pathogenesis using structure-based site-directed mutagenesis of gH. The distal tip of domain (D)I was important for skin tropism, entry, and fusion. DII helices and a conserved disulfide bond were essential for gH structure and VZV replication. An essential ^{724}CXXC^{727} motif was critical for DIII structural stability and membrane fusion. This assignment of domain-dependent mechanisms to VZV gH links elements of the glycoprotein structure to function in herpesvirus replication and virulence.

Herpesviruses are ubiquitous and important pathogens in both immunocompetent and immunocompromised individuals. Three of the eight human herpesviruses, varicella-zoster virus (VZV) and herpes simplex viruses 1 and 2 (HSV-1 and HSV-2), are α-herpesviruses (1). These three viruses initiate infection at mucosal sites. The pathogenesis of primary VZV infection, varicella (chicken pox), then depends on T-cell infection, which transfers VZV to skin and results in the establishment of latency in the sensory nerve ganglia (2). VZV skin lesions consist of polykaryocytes that are generated by cell fusion and release large quantities of virus. In contrast, VZV infection does not induce T-cell fusion, allowing these cells to transport virus to skin and neurons. VZV reactivation from latency causes zoster (shingles) and the debilitating condition postherpetic neuralgia.

After host cell attachment, entry by enveloped viruses, including herpesviruses, requires fusion. Enveloped viruses typically use a single fusogenic glycoprotein, but evidence from several herpesviruses indicates that entry fusion is induced by a multiprotein core complex consisting of glycoprotein (g)B and the heterodimer gH/gL (3). gH requires the scaffolding protein gL for maturation and transport, although gL might also promote fusion (4–6). The gH homologs of HSV-1, Epstein–Barr virus (EBV) and pseudorabies virus (PRV), are required for virus entry (7–9). VZV gH and gL are essential for virus replication, and antibodies to gH inhibit both VZV entry and cell fusion (10, 11). Despite extensive evidence that herpesvirus gH proteins are an essential component of the fusion complex, how gH/gL proteins function in fusion has yet to be fully elucidated.

gH was originally proposed to act directly as a fusogen, but the newly resolved crystal structures of HSV-2 and EBV gH/gL and PRV gH do not resemble known viral fusion proteins (12–14). HSV-2 gH/gL forms a "boot-like" structure with three distinct domains. The gH N-terminal domain (D)I is composed of β-sheets that cofold with gL, the central helical DII contains 16 α-helices, and the C-terminal DIII forms a highly conserved β-sandwich. EBV and PRV gH/gL structures have been divided into four domains rather than the three proposed for HSV gH (12–14). The overall structures are comparable, although EBV gH/gL form a rod-like structure due to disparate interdomain packing angles. The PRV gH structure lacks the N terminus and gL but shows similar architecture in the regions classified as DII and DIII in HSV gH (12, 13).

Previous studies of gH/gL using expression vectors and complementation assays demonstrate that HSV-1 and EBV gH regions now mapped to DI have functions in fusion and integrin binding (6, 15–17). Heptad repeats predicted to form coiled-coils and hydrophobic α-helices that interact with membranes identified in HSV-1 gH DII are typical elements of class I fusion proteins, but the structural analysis shows they are buried within DII and unlikely to act as fusion peptides (13, 18–20). Two disulfide bonds, confirmed in the HSV-2 gH crystal structure, are required for HSV-1 and HSV-2 gH function in vitro (21).

This study exploits new knowledge about gH/gL structure to define the specific functions of gH domains. The approach uses VZV gH as a representative of this highly conserved protein in the *Herpesviridae* because site-directed mutagenesis of the gene can be done in the VZV genome and function can be evaluated not only in vitro but also in vivo in human skin xenografts in the SCID mouse model of VZV pathogenesis (22). The similarities of gH in VZV and HSV-2 (23) enabled domain modeling from the HSV gH/gL structure. Mutations were introduced into ORF37, which encodes gH, of the VZV genome to determine their effects on viability and replication in vitro and skin infection in vivo. Domains were further characterized using a cell fusion assay and virus entry into T cells. Specific gH domains had functions in skin tropism, maintaining the gH structure required for viral replication and cell fusion necessary for virulence in skin. The biological significance of gH DIII-dependent cell fusion was unequivocally demonstrated by a mutation that evolved through natural selection in skin, rescuing defective fusion and replication caused by mutagenesis of the ^{724}CXXC^{727} motif. Thus, the disulfide bonds and bridging strand were shown to be essential for the structural stability of DIII, which mediates gH-dependent fusion in the *Herpesviridae*.

Results

Homology Modeling of VZV gH. VZV gH was modeled on the crystal structures of the α-herpesviruses HSV-2 and PRV and the γ-herpesvirus EBV (Fig. 1, Fig. S1, Movie S1, and Table S1). The VZV gH structure based on HSV-2 gH had a single gap in

Author contributions: S.E.V., S.L.O., and A.M.A. designed research; S.E.V., S.L.O., J.J.B., and J.R. performed research; S.E.V., S.L.O., J.J.B., H.M.B., and M.H.S. contributed new reagents/analytic tools; S.E.V. and S.L.O. analyzed data; and S.E.V., S.L.O., and A.M.A. wrote the paper.

The authors declare no conflict of interest.

This article is a PNAS Direct Submission.

[1]S.E.V. and S.L.O. contributed equally to this work.

[2]To whom correspondence should be addressed. E-mail: sevleck@stanford.edu.

This article contains supporting information online at www.pnas.org/lookup/suppl/doi:10.1073/pnas.1111333108/-/DCSupplemental.

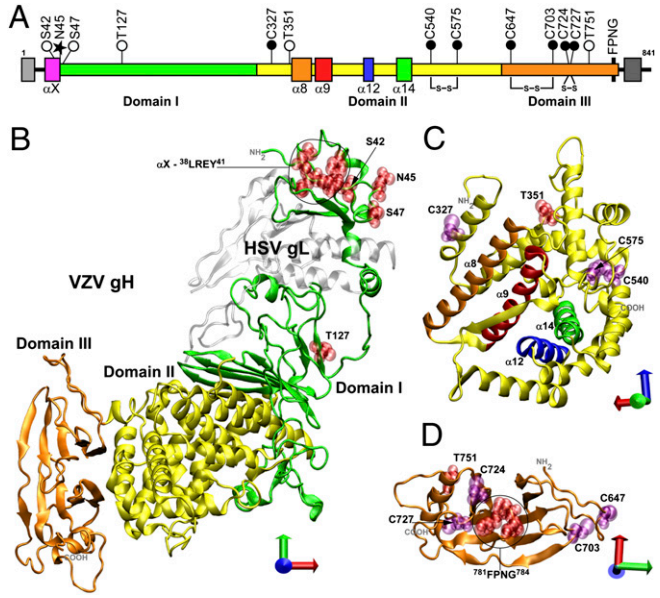

Fig. 1. The localization of site-directed mutagenesis in the homology model of VZV gH. (*A*) Linear diagram of gH depicting targeted mutations. Signal sequence, light gray box; DI, green; DII, yellow; DIII, orange; αX, pink box; serine and threonine, white circles; glycosylation site, black star; cysteines, black circles; α8, orange box; α9, red box; α12, blue box; α14, green box; FPNG, black bar; transmembrane region, dark gray box. Predicted disulfide bonds are connected with lines. (*B*) The complete VZV gH homology model based on HSV-2 gH, shown with HSV gL (silver). (*C*) Domain II of VZV gH. (*D*) Domain III of VZV gH. (*B–D*) Locations of substitutions are depicted in red or purple space fill. Axes: *x*, red; *y*, green; *z*, blue.

the amino acid alignment of more than five residues, whereas alignment with PRV or EBV gH had several large gaps in the putative DII. VZV gL could not be modeled due to low identity with HSV and EBV gL.

The ^{38}LREY^{41} (αX) residues in VZV gH DI formed a predicted γ-turn in the homology model (Fig. 1 *A* and *B*), stabilized by an R39–Y41 hydrogen bond. These residues are at the extreme N terminus of DI encompassed by the alignment with HSV, in a position analogous to a bioinformatically predicted α-helix with heptad-repeat characteristics (24). The β-sheet that curves around the central helical domain in HSV-2 was conserved in the VZV gH model. The disulfide bond between DI and DII in HSV-2 gH was not conserved, as cysteines are absent in VZV gH DI, and VZV gH DII C327 was not in close proximity to any other gH cysteine. The central helical domain (DII) of the VZV gH model consisted of 12 α-helices and four 3_{10}-helices, mirroring those in HSV-2 gH. This tight helical bundle encompassed structures that were reminiscent of heptad-repeat coiled-coils, which were packed tightly with numerous interhelix interactions. A disulfide bond between C540 and C575 in VZV gH was similar to one conserved in HSV-2. The VZV model predicts a DIII β-sandwich configuration similar to DIII of HSV-2, PRV, and EBV gH, which is the most conserved gH domain. Two five-stranded β-sheets fold to form a core with extended loops connecting the β-strands. The central portion of the β-sandwich envelopes the residues ^{781}FPNG^{784}, which form a type I hydrogen-bonded β-turn in the homology model and are highly conserved across the α-herpesviruses. Similar to HSV-2, the VZV gH model predicts a conserved disulfide bond between C674 and C703. VZV gH is also highly likely to have a second disulfide bond between C724 and C727, comparable to PRV and EBV gH. This ^{724}CXXC^{727} motif is conserved across the *Herpesviridae* except for the simplexviruses.

Domain I Functions in VZV Skin Tropism and Pathogenesis in Vivo. The function of the predicted γ-turn ^{39}REY^{41} in αX was investigated by glycine substitutions to generate ^{38}GRGG^{41}, simultaneously abolishing the γ-turn and the heptad repeat (Fig. 1). The function of a predicted *N*-linked glycosylation motif NX[ST] at ^{45}NMS^{47} was investigated by alanine substitution of N45 or S47. A threonine substitution of S47 was used as a control to maintain the glycosylation motif. Residue S42 was substituted with alanine to establish that point mutations in this region did not affect gH function. A spontaneous T127A substitution occurred during cloning. Two alanine substitutions at T351, between helices α7 and α8, and C327, the first cysteine residue in VZV gH, were also tested. These two residues are in DII but are found at the DI–DII interface and were grouped with the DI substitutions. Viable viruses were recovered that had each of these mutations (Tables S2 and S3).

The localization of gH was unaffected in cells infected with each of the DI mutants with the exception of αX (Fig. 2*A* and Fig. S2*A*). Strikingly, although αX plaque formation was unaltered, the anti-

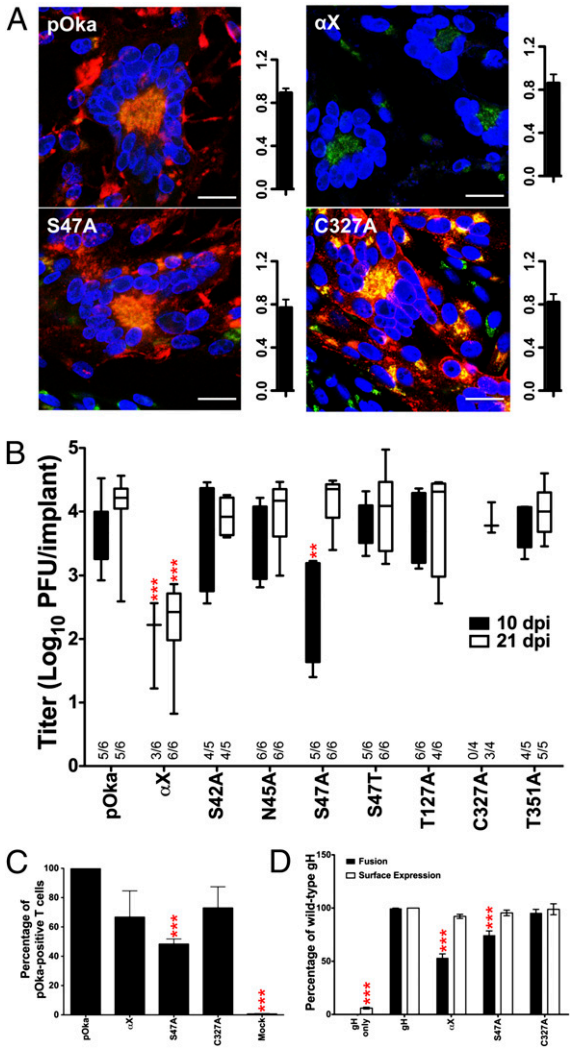

Fig. 2. DI mutants disrupt skin pathogenesis by reducing fusion and cell entry. (*A*) Confocal microscopy and plaque size (mm^2) of pOka, αX, S47A, and C327A in infected cells. gH, red; trans-Golgi network (TGN), green; nuclei, blue. (Scale bars, 25 μm.) (*B*) In vivo replication at 10 and 21 dpi. Xenografts positive for infectious virus out of total xenografts inoculated are indicated on the *x* axis. (*C*) T-cell entry of gH mutants αX, S47A, and C327A relative to pOka. (*D*) Cell fusion and surface expression of αX, S47A, and C327A relative to gH. Mean ± SEM. $^{**}P < 0.01$, $^{***}P < 0.001$.

gH mAb SG3 was unable to detect αX gH, suggesting a change in gH epitope conformation or accessibility. Maturation of gH in wild-type pOka-infected cells produces immature (100-kDa) and two mature (118- and 130-kDa) protein species (Fig. S2*B*). gH maturation was unaffected by the DI mutations, although, consistent with confocal data, αX gH was not detected. The *N*-linked glycosylation site at ^{45}NMS^{47} was confirmed by the ∼5-kDa reduction in M_r for all gH protein species from N45A and S47A, whereas S47T was similar to WT gH. Importantly, expression of VZV proteins representing the immediate-early (IE63), early (capsid protein ORF23), and late (gE) classes was similar to pOka in cells infected with DI mutants, including αX (Fig. S2*C*). Thus, altered gH structure in αX and the lack of glycosylation at N45 did not adversely affect viral protein expression.

In vitro replication kinetics and plaque sizes for all of these mutants were similar to pOka (Fig. 2*A* and Fig. S2 *A* and *D*). In contrast, αX and S47A significantly impaired replication in human skin in vivo (Fig. 2*B*). αX titers in skin were significantly reduced compared with pOka at 10 and 21 d postinfection (dpi), implicating ^{38}LREY^{41} in skin tropism. S47A replication was delayed, with significantly lower titers only at 10 dpi. The loss of N45 glycosylation did not account for the defective S47A replication because N45A and S47T replication was similar to pOka, indicating that a hydroxyl moiety at residue 47 is required for gH function. Virus was not detected at 10 dpi in C327A-inoculated skin, but titers were equivalent to pOka at 21 dpi.

To determine whether impaired skin virulence of αX, S47A, or C327A was caused by decreased entry or cell fusion, mutants were tested for these functions. T-cell entry of αX or C327A was not significantly reduced, but S47A entry was severely impaired (Fig. 2*C*). αX and to a lesser extent S47A significantly reduced membrane fusion, but C327A had no effect (Fig. 2*D*). Importantly, cell surface expression of the mutated proteins was comparable to WT gH. Thus, reduced skin pathogenicity of the αX virus was attributable to diminished cell fusion, whereas the S47A virus was impaired for both entry and fusion.

Antibody binding studies provided evidence that reduced αX fusion and skin pathogenicity were attributable to altered gH structure. In infected cells, mAb 206 detected αX gH weakly, whereas mAb 258, like SG3, did not bind gH (Figs. 2*A* and 3*A*).

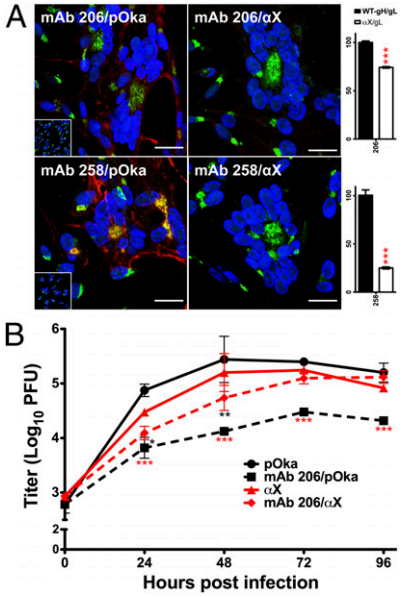

Fig. 3. Structural alterations within αX disrupt binding of neutralizing antibodies. (*A*) Confocal microscopy of pOka- and αX-infected cells using mAbs 206 and 258. gH, red; TGN, green; nuclei, blue. (Scale bars, 25 μm.) (*Right*) Quantification of gH detection in transfected cells. (*B*) VZV neutralization assay using mAb 206. Mean ± SEM. *$P < 0.05$, **$P < 0.01$, ***$P < 0.001$.

All three anti-gH neutralizing antibodies had reduced affinity for αX gH in transfected cells (Fig. 3*A* and Fig. S3 *A* and *B*). αX neutralization by mAb 206 was significantly reduced compared with pOka (Fig. 3*B*), consistent with decreased antibody affinity for αX gH. Thus, the gH N terminus contains epitopes recognized by conformation-dependent neutralizing antibodies. Although maintained in transfected cells, the αX gH DI conformation was altered to mask these epitopes in infected cells. These data strongly support a role for binding of the distal region of gH to a cellular receptor(s) that is required for VZV skin tropism and fusion but not replication in vitro.

Domain II Structure Is Critical for gH Localization and Maturation. To determine the role of the DII helical bundle, four α-helices and a disulfide bond were disrupted (Fig. 1 *A* and *C*). The highly hydrophobic helices α8 and α14 were kinked by introducing prolines (^{368}AARIA^{372} to PPRIP; ^{505}LFFA^{508} to DPPD). Helices α9 and α12 were disrupted by abolishing predicted coiled-coil formation but not the helix (^{399}QL^{400} to AA; ^{456}DEARDQL^{462} to AAARDQA). The C540–C575 predicted disulfide bond was disrupted by alanine substitution. All DII mutations were lethal for VZV replication (Table S2). Lethality was not caused by secondary mutations in the VZV genome, as viable virus was recovered when the mutant ORF37 was replaced with WT.

gH trafficking to the cell surface was partially or completely prevented by all DII mutations (Fig. 4 and Fig. S4*A*). All DII mutants were detected in permeabilized cells, confirming their expression and detection by SG3. In nonpermeabilized cells, α9 and α12 mutants had a significantly reduced, patchy distribution along the cell surface, whereas the remaining DII mutants were not detected. Three gH protein species were detected in cells transfected with gH and gL (Fig. S4*B*). In contrast, only the 100-kDa gH was detected in α8, α9, α12, C540A, and C575A transfected cells, suggesting that disrupted gH processing might lead to rapid gH degradation. Thus, the DII helices and disulfide bond are vital to gH structure and absolutely required for gH maturation and trafficking necessary for viral replication.

As anticipated, DII mutants absent from the cell surface failed to induce fusion (Fig. 4). The patchy surface expression of α9 and α12 was also insufficient for membrane fusion. The expectation that the α9 and α12 mutants maintained a helical structure was tested using mimetic peptides. The spectra for the WT and mutant α12 peptides suggested a random-coil conformation in buffer alone (Fig. S4*C*). Both peptides formed robust helices in trifluoroethanol concentrations ≥40%, which mimics a hydrophobic environment, suggesting that the α12 mutation did not affect α-helix formation but altered side-chain interactions with other DII helices. Experiments with the α9 peptides were not possible due to their extreme hydrophobicity.

Domain III Functions in Membrane Fusion and Virulence in Human Skin. To determine their role in gH function, the DIII disulfide bonds C647–C703 and C724–C727 were disrupted by alanine substitution (Fig. 1 *A* and *D*), allowing simultaneous assessment of the disulfide bonds and the ^{724}CXXC^{727} motif. This motif has been

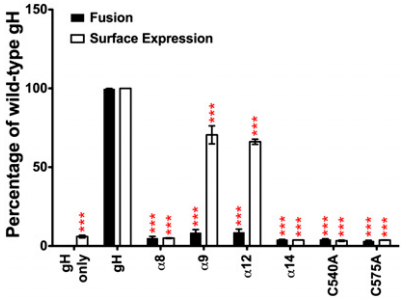

Fig. 4. DII mutants disrupt or abolish gH fusion. Cell fusion and surface expression of DII mutants relative to gH. Mean ± SEM. ***$P < 0.001$.

proposed to function as a protein disulfide isomerase (12). The function of the conserved residues ^{781}FPNG^{784} that form a predicted type I β-turn at the β-sandwich core was also assessed via alanine substitutions, as was residue T751 within α22, the only predicted α-helix of DIII. The C724A and FPNG (^{781}AAAA^{784}) mutations were lethal for VZV replication but could be rescued by substituting the mutated gene with WT ORF37, whereas the remaining mutations all produced viable virus (Table S2).

Similar to the lethal DII mutants, ^{781}FPNG^{784} gH was not detected on the cell surface and could not be immunoprecipitated from transfected cells (Fig. S5 *A* and *C*). Thus, the β-turn was critical for the DIII structure required for gH transport and production of infectious virions. In contrast to FPNG, C724A surface expression was significantly reduced in transfected cells but was not statistically different from C727A expression, whereas maturation was similar to WT gH and all three C724A protein species were detected. This suggested that C724A lethality was not a consequence of altered gH maturation or surface expression but instead directly disrupted an essential gH fusion function (see below).

The viable C647A, C703A, and C727A mutants all had significantly reduced syncytia formation and plaque size compared with pOka (Fig. 5*A* and Fig. S5*B*). gH expression was reduced, contributing to the decreased syncytia formation and plaque size. The 100-kDa protein was the only gH species detected in C647A-, C703A-, and C727A-infected cells, consistent with the limited gH expression observed by confocal microscopy (Fig. S5*B*). However, cell surface detection of these mutants suggested that gH maturation occurred (Fig. 5*D*). Similarly, the T751A virus had significantly reduced plaque size but the phenotype was less severe. Maturation of T751A gH was typical but expression was diminished, suggesting more rapid degradation. Importantly, expression levels of IE63, ORF23, and gE were not deficient in any of the DIII viable mutants compared with pOka (Fig. S5*E*).

T751A replication in vitro did not differ from pOka, and the small-plaque phenotype did not translate to reduced skin virulence in vivo (Fig. 5*B* and Fig. S5*F*). In contrast, the in vitro replication kinetics of the C647A, C703A, and C727A viruses were significantly reduced, as was virulence in human skin, demonstrating the importance of the DIII disulfide bonds in gH function during VZV replication in differentiated skin tissue.

All viable DIII mutants retained the capacity for T-cell entry, but functional defects were identified for membrane fusion (Fig. 5 *C* and *D*). The ^{781}FPNG^{784} mutant was not expressed on the cell surface and consequently failed to induce fusion. T751A had surface expression equivalent to gH but exhibited reduced fusion, consistent with the diminished ability of this virus to form large syncytia in vitro. Disulfide-bond disruption in DIII abolished fusion, consistent with the in vitro and in vivo phenotypes of the C647A, C703A, and C727A viruses and the lethality of the C724A mutation. Thus, DIII structural integrity requires these cysteines for gH-mediated fusion associated with VZV skin pathogenesis.

Naturally Occurring Mutation S694F Within DIII Rescued the C724A and C727A Phenotypes. Replication of the C727A virus in skin was unexpectedly robust at 10 dpi compared with the other cysteine mutants (Fig. 5*B*). Surprisingly, virus recovered from skin produced plaque morphologies similar to pOka (Fig. 6*A*), suggesting that a compensatory mutation had evolved. The expected C727A mutation and a new mutation, S694F, were identified in all isolates recovered from skin. The S694F mutation was not detected in early passages of C727A (Fig. 6*B*), which were used for in vitro assays, but was identified in retrospect as a very minor population in late passages used to inoculate skin. By 10 dpi, the double mutant S694F/C727A was the dominant virus. The single C727A mutant virus could not be detected at 21 dpi.

The S694F/C727A virus had replication kinetics and plaque sizes similar to pOka, whereas the C727A virus was deficient (Fig. 6 *A* and *C*). T-cell entry was unaffected (Fig. 6*D*). To confirm the S694F phenotype, S694F was incorporated into the C724A or C727A constructs. Cell fusion was restored in both mutants, although to a lesser extent for C724A (Fig. 6*E*). Importantly, the lethal phenotype of the C724A mutation was rescued by incorporating S694F into the C724A BAC. The compensatory effect of S694F demonstrated that the ^{724}CXXC^{727} disulfide bond functions to stabilize DIII structure.

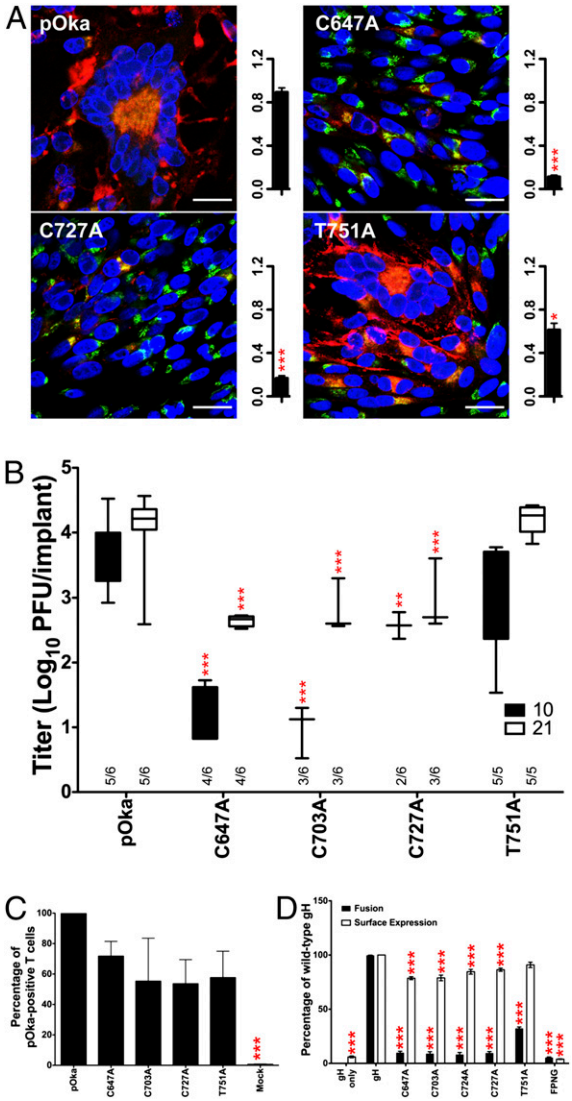

Fig. 5. DIII mutants reduce skin pathogenesis by disrupting fusion. (*A*) Confocal microscopy and plaque size (mm^2) of pOka, C647A, C727A, and T751A in infected cells. gH, red; TGN, green; nuclei, blue. (Scale bars, 25 μm.) (*B*) In vivo replication at 10 and 21 dpi. Xenografts positive for infectious virus out of total xenografts inoculated are indicated on the *x* axis. (*C*) T-cell entry of DIII viable mutants relative to pOka. (*D*) Cell fusion and surface expression of all DIII mutants relative to gH. Mean ± SEM. *$P < 0.05$, **$P < 0.01$, ***$P < 0.001$.

Discussion

Recent advances revealing the structure of the highly conserved herpesvirus gH/gL proteins were the foundation for these experiments to link gH domains I, II, and III with their functions. Site-directed mutagenesis of VZV gH allowed the identification of domain-specific structural determinants required for viral replication, cell fusion, and skin tropism.

DI, implicated here in skin tropism, has the most variable amino acid sequence within herpesvirus gH proteins, indicating its independent evolution in each subfamily (25). The dependence of gH on gL for protein folding and their coevolution may contribute to DI structural variation (13). Herpesviruses target specific dif-

MICROBIOLOGY

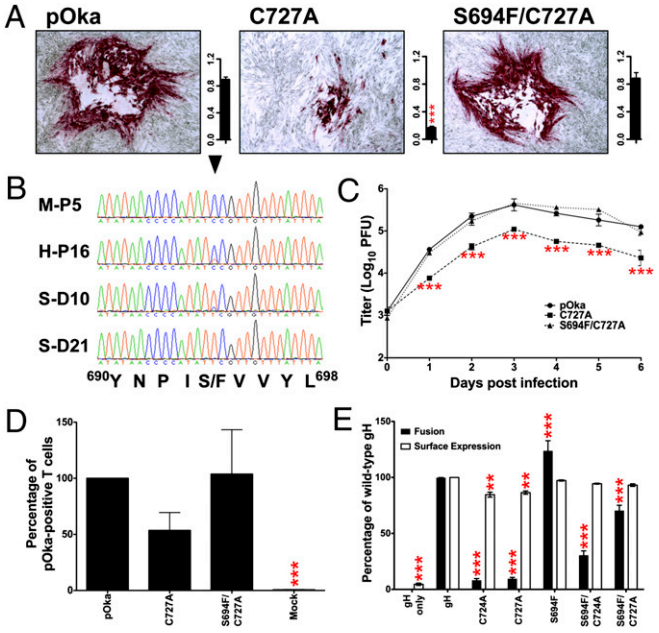

Fig. 6. The S694F mutation compensates for C724A and C727A phenotypes. (*A*) Plaque formation and size (mm^2) of pOka, C727A, and S694F/C727A in infected cells. (*B*) Chromatograms of C727A virus sequence in melanoma cells (M-P5), fibroblasts (H-P16), and representative 10- and 21-dpi skin (S-D10/21). The arrowhead indicates the TYC nucleotides that encode S/F694. (*C*) In vitro replication kinetics. (*D*) T-cell entry of C727A and S694F/C727A relative to pOka. (*E*) Cell fusion and surface expression of C724A, C727A, S694F, S694F/C724A, and S694F/C727A relative to gH. Mean ± SEM. $^{**}P < 0.01$, $^{***}P < 0.001$.

ferentiated cell types during replication in the natural host, and differences in gH cellular receptors probably also account for DI variability. In VZV gH, the distal tip of DI mediated skin tropism by two distinct mechanisms relating to cell fusion and virus entry. Whereas the S47A change had a marked effect on entry, the subtle alteration of the αX gH structure was associated with impaired cell fusion and replication in skin. From these observations, skin and T cells would be predicted to have different host cell proteins that interact with VZV gH/gL, and interactions with the αX region may contribute directly to skin tropism.

gH interactions with viral or cellular proteins have been proposed to modulate cell tropism in other herpesviruses (26–28). EBV has differential requirements for infection of epithelial cells or B cells in vitro (29). An L65A substitution in EBV gH reduces cell fusion and significantly reduces binding of mAb E1D1 (16). Unlike the VZV αX and S47A substitutions, EBV gH L65 is at the hydrophobic interface between gH DI and gL, and L65A appears to disrupt gH/gL cofolding, destabilizing the region and reducing maturation and trafficking to the cell surface (14, 30). In contrast, all of the VZV gH DI mutants matured and trafficked properly, demonstrating that gH–gL interactions were unaffected. Thus, the prominent effect of the disrupted γ-turn in the αX mutant on skin virulence implicates this extreme N terminus of gH/gL in skin tropism relating to cell fusion but not entry, possibly through interactions with cell proteins required for fusion between infected and uninfected skin cells.

The S47 residue appears to be more important for entry than cell fusion. Inefficient entry accounts for the poor initial replication of S47A in skin, whereas relatively intact cell fusion enabled the virus to replicate and spread throughout the skin to WT levels by 21 dpi. This function can be linked to the hydroxyl group at this gH residue because S47T and N45A did not have any effect on gH function and, importantly, did not impair skin pathogenesis in vivo. DI of HSV gH interacts with αvβ3 integrin, potentially facilitating virus entry (15, 31). Similarly, EBV gH interacts with αvβ6/8 integrins, and the EBV gH/gL structure suggests multiple contacts with DI residues (14, 17). Interactions between VZV gH and integrins would likely occur in a similar manner to EBV gH, possibly involving the outward-facing hydroxyl group of S47 (Fig. S2*E*). Losing the hydroxyl group would reduce binding affinity during attachment, thereby reducing entry efficiency and impairing the initial replication of VZV in skin in vivo.

This study identifies the DII helical bundle structure as necessary for gH maturation and cell surface expression, which are required for viral replication and cell fusion. Previous studies, published before the gH/gL structures were reported, associated DII with cell fusion. These analyses, based on linker insertion mutagenesis, grossly affected the DII structure (32, 33). Other studies using targeted mutations in the homologous HSV helices have suggested these helices act as fusion peptides and play a direct role in fusion (19). However, the HSV-2 gH/gL structure places these helices at the core of DII, where they are inaccessible as fusion peptides (13). Similarly, helices in HSV gH homologous to VZV gH α9 and α12 have been suggested to function as heptad repeats that aid in conformational change during fusion (20, 24). These helices are also buried inside the DII helical bundle and are unlikely to promote any substantial conformational changes. The present study demonstrates that α-helices, including minor interactions among helices in DII, such as those mimicking coiled-coil interactions of heptad repeats, are essential for maintaining gH architecture rather than having direct roles in gH fusion.

DIII is the most conserved gH domain based on sequence and from structural studies. Insertions or point mutations in the DIII β-sheets of EBV gH and substitution of the two cysteines in HSV-1 and HSV-2 gH expression constructs disrupted fusion in cell-based fusion assays (21, 34, 35). Mutation of the conserved ^{781}[FY]PNGT^{785} DIII motif was lethal for VZV replication. This motif contains an *N*-linked glycosylation site motif, NX[ST], and is glycosylated in HSV-2 gH at N784, but this glycosylation was dispensable for HSV replication (13, 32). The VZV gH homology model and the lethality of the FPNG mutant suggest that the conserved ^{781}[FY]PNGT^{785} sequence stabilizes DIII by forming a type I β-turn between β21 and β22 at the core of the β-sandwich. Without this stability, gH transport to cell surfaces is abolished, demonstrating that the structural integrity of the β-sandwich is vital for gH function.

The two predicted disulfide bonds C647–C703 and C724–C727 in VZV gH DIII bracket a bridging strand, which was designated a "flap" in PRV (12). The bridging strand, formed by β17 and β18, is vital for EBV fusion, as demonstrated by insertions or point mutations that abolished cell fusion or fusion specific to epithelial or B cells (34, 35). Furthermore, an antibody to the EBV gH bridging strand can neutralize fusion (36). However, before this analysis of VZV gH, the role of cysteines in bridging-strand function was unclear. The PRV CXXC motif, conserved throughout the *Herpesviridae* with the exception of the simplexviruses, was suggested to provide flexibility for the bridging strand to move, exposing a hydrophobic patch during fusion (12). In VZV, mutations that disrupted either disulfide bond abolished gH-mediated cell fusion. Modeling the increased flexibility through loss of the disulfide bonds predicted reduced interactions between the bridging strand and β-strands within the DIII β-sandwich, which could expose a hydrophobic patch, as suggested for PRV. Rather than aiding gH function, this predicted flexibility decreased the overall stability of DIII required for membrane fusion and efficient viral pathogenesis, suggesting that DIII rigidity, not flexibility, is a major requirement for gH functions.

Direct evidence for the importance of gH DIII rigidity was provided by the S694F mutation at the second residue in β16, which evolved naturally to rescue gH function. The bulky phenylalanine residue potentially induced expansion at the core of DIII, instigating global changes in side-chain interactions that could compensate for the reduced rigidity caused by the C724A and C727A substitutions. Comparisons of VZV gH DIII homology models demonstrated this potential (Fig. S6). In the homology

models of WT and C727A gH/gL, S694 lies in close proximity to K675 and S683. However, in S694F/C727A, the bulky aromatic group on the phenylalanine causes a substantial reorientation of K675. This change in the model brings K675 into close proximity to S705 in the bridging strand, suggesting that stabilizing interactions occur with the bridging strand despite the loss of the C724–C727 disulfide bond. In support of this hypothesis, the homology model movement of K675 was less pronounced in C724A, providing an explanation for the partial fusion rescue with S694F/C724A compared with the complete fusion rescue with S694F/C727A. Thus, the effects of the S694F mutation provide compelling evidence that the ^{724}CXXC^{727} motif performs a critical stabilizing role for this highly conserved gH domain.

The S694F/C727A mutant emerged as the single VZV genotype under selective pressure during VZV replication in vivo, proving the fundamental importance of gH-dependent cell fusion in skin pathogenesis. This observation also provides a valuable insight into gH-dependent fusion in the simplexviruses. HSV-1 and HSV-2, which have the homologous C647–C703 disulfide bond, also have a phenylalanine in the position homologous to VZV gH S694. This residue would be predicted to compensate for the absence of the CXXC motif in these viruses. A linker insertion in HSV gH with close proximity to this phenylalanine abolished syncytia formation, supporting the concept that structural rigidity of this region is required for HSV gH function (32). All other human herpesviruses have the two homologous gH DIII disulfide bonds, and the human γ-herpesviruses have a homologous phenylalanine, indicating that the structural rigidity and functions mapped to the gH bridging-strand structure in VZV are preserved across the *Herpesviridae*.

This extensive analysis demonstrates that gH is a critical determinant of herpesvirus-induced fusion in vitro and in vivo, even though recent structural analyses of HSV-2, PRV, and EBV gH/gL show no similarities to viral fusogens (12–14). Specific DI residues in the N terminus support virus entry as well as cell fusion, thereby mediating skin tropism. DII is essential for gH maturation and cell surface expression, which is necessary for all gH functions and virus replication. Cell fusion is highly dependent on the integrity of the DIII bridging strand and the resulting stability of DIII. Its extreme conservation indicates evolutionary preservation of a structure essential to the role of gH in the gB/gH/gL fusion machinery across the *Herpesviridae*.

Methods

Detailed methods are provided in *SI Methods*. These describe cells, viruses, proteins, plasmids, in vitro replication, in vivo pathogenesis, T-cell entry, and cell fusion, as well as statistical methods. Newly developed research materials and assays include the rabbit polyclonal antibody against VZV gH and the cell-based fusion assay.

ACKNOWLEDGMENTS. We acknowledge Tadahiro Suenaga and Hisashi Arase, Osaka University, and Yasuko Mori, National Institute of Biomedical Innovation, and Kobe University Graduate School of Medicine, for providing fusion assay plasmids; Klaus Osterrieder, Freie Universität, for providing the VZV pOka BAC; Ruth Sommese and James Spudich, Stanford University, for assistance with circular dichroism; and Hisae Matsuura and Theodore Jardetzky, Stanford University, for insightful discussion regarding EBV and VZV gH structure. Funding was provided by National Institutes of Health Grants AI20459, GM007279, and AI007328.

1. Pellett PE, Roizman B (2007) The family *Herpesviridae*: A brief introduction. *Fields Virology*, eds Knipe DM, et al. (Lippincott-Williams &Wilkins, Philadelphia), 5th Ed, pp 2479–2499.
2. Cohen JI, Straus SE, Arvin AM (2007) Varicella-zoster virus replication, pathogenesis and management. *Fields Virology*, eds Knipe DM, et al. (Lippincott-Williams & Wilkins, Philadelphia), 5th Ed, pp 2773–2818.
3. Connolly SA, Jackson JO, Jardetzky TS, Longnecker R (2011) Fusing structure and function: A structural view of the herpesvirus entry machinery. *Nat Rev Microbiol* 9:369–381.
4. Plate AE, Smajlović J, Jardetzky TS, Longnecker R (2009) Functional analysis of glycoprotein L (gL) from rhesus lymphocryptovirus in Epstein-Barr virus-mediated cell fusion indicates a direct role of gL in gB-induced membrane fusion. *J Virol* 83: 7678–7689.
5. Duus KM, Grose C (1996) Multiple regulatory effects of varicella-zoster virus (VZV) gL on trafficking patterns and fusogenic properties of VZV gH. *J Virol* 70:8961–8971.
6. Cairns TM, et al. (2007) N-terminal mutants of herpes simplex virus type 2 gH are transported without gL but require gL for function. *J Virol* 81:5102–5111.
7. Forrester A, et al. (1992) Construction and properties of a mutant of herpes simplex virus type 1 with glycoprotein H coding sequences deleted. *J Virol* 66:341–348.
8. Oda T, Imai S, Chiba S, Takada K (2000) Epstein-Barr virus lacking glycoprotein gp85 cannot infect B cells and epithelial cells. *Virology* 276:52–58.
9. Peeters B, de Wind N, Broer R, Gielkens A, Moormann R (1992) Glycoprotein H of pseudorabies virus is essential for entry and cell-to-cell spread of the virus. *J Virol* 66: 3888–3892.
10. Zhang Z, et al. (2010) Genome-wide mutagenesis reveals that ORF7 is a novel VZV skin-tropic factor. *PLoS Pathog* 6:e1000971.
11. Vleck SE, et al. (2010) Anti-glycoprotein H antibody impairs the pathogenicity of varicella-zoster virus in skin xenografts in the SCID mouse model. *J Virol* 84:141–152.
12. Backovic M, et al. (2010) Structure of a core fragment of glycoprotein H from pseudorabies virus in complex with antibody. *Proc Natl Acad Sci USA* 107:22635–22640.
13. Chowdary TK, et al. (2010) Crystal structure of the conserved herpesvirus fusion regulator complex gH-gL. *Nat Struct Mol Biol* 17:882–888.
14. Matsuura H, Kirschner AN, Longnecker R, Jardetzky TS (2010) Crystal structure of the Epstein-Barr virus (EBV) glycoprotein H/glycoprotein L (gH/gL) complex. *Proc Natl Acad Sci USA* 107:22641–22646.
15. Parry C, Bell S, Minson T, Browne H (2005) Herpes simplex virus type 1 glycoprotein H binds to αvβ3 integrins. *J Gen Virol* 86:7–10.
16. Omerović J, Lev L, Longnecker R (2005) The amino terminus of Epstein-Barr virus glycoprotein gH is important for fusion with epithelial and B cells. *J Virol* 79: 12408–12415.
17. Chesnokova LS, Nishimura SL, Hutt-Fletcher LM (2009) Fusion of epithelial cells by Epstein-Barr virus proteins is triggered by binding of viral glycoproteins gHgL to integrins αvβ6 or αvβ8. *Proc Natl Acad Sci USA* 106:20464–20469.
18. Galdiero S, et al. (2005) Fusogenic domains in herpes simplex virus type 1 glycoprotein H. *J Biol Chem* 280:28632–28643.
19. Gianni T, Fato R, Bergamini C, Lenaz G, Campadelli-Fiume G (2006) Hydrophobic α-helices 1 and 2 of herpes simplex virus gH interact with lipids, and their mimetic peptides enhance virus infection and fusion. *J Virol* 80:8190–8198.
20. Gianni T, Piccoli A, Bertucci C, Campadelli-Fiume G (2006) Heptad repeat 2 in herpes simplex virus 1 gH interacts with heptad repeat 1 and is critical for virus entry and fusion. *J Virol* 80:2216–2224.
21. Cairns TM, Landsburg DJ, Whitbeck JC, Eisenberg RJ, Cohen GH (2005) Contribution of cysteine residues to the structure and function of herpes simplex virus gH/gL. *Virology* 332:550–562.
22. Moffat JF, et al. (1998) The ORF47 and ORF66 putative protein kinases of varicella-zoster virus determine tropism for human T cells and skin in the SCID-hu mouse. *Proc Natl Acad Sci USA* 95:11969–11974.
23. McGeoch DJ, Dolan A, Ralph AC (2000) Toward a comprehensive phylogeny for mammalian and avian herpesviruses. *J Virol* 74:10401–10406.
24. Gianni T, Menotti L, Campadelli-Fiume G (2005) A heptad repeat in herpes simplex virus 1 gH, located downstream of the α-helix with attributes of a fusion peptide, is critical for virus entry and fusion. *J Virol* 79:7042–7049.
25. McGeoch DJ, Davison AJ (1986) DNA sequence of the herpes simplex virus type 1 gene encoding glycoprotein gH, and identification of homologues in the genomes of varicella-zoster virus and Epstein-Barr virus. *Nucleic Acids Res* 14:4281–4292.
26. Wang D, Shenk T (2005) Human cytomegalovirus virion protein complex required for epithelial and endothelial cell tropism. *Proc Natl Acad Sci USA* 102:18153–18158.
27. Wang X, Kenyon WJ, Li Q, Müllberg J, Hutt-Fletcher LM (1998) Epstein-Barr virus uses different complexes of glycoproteins gH and gL to infect B lymphocytes and epithelial cells. *J Virol* 72:5552–5558.
28. Mori Y, et al. (2004) Discovery of a second form of tripartite complex containing gH-gL of human herpesvirus 6 and observations on CD46. *J Virol* 78:4609–4616.
29. Li Q, Turk SM, Hutt-Fletcher LM (1995) The Epstein-Barr virus (EBV) BZLF2 gene product associates with the gH and gL homologs of EBV and carries an epitope critical to infection of B cells but not of epithelial cells. *J Virol* 69:3987–3994.
30. Pulford DJ, Lowrey P, Morgan AJ (1995) Co-expression of the Epstein-Barr virus BXLF2 and BKRF2 genes with a recombinant baculovirus produces gp85 on the cell surface with antigenic similarity to the native protein. *J Gen Virol* 76:3145–3152.
31. Gianni T, et al. (2010) Herpes simplex virus glycoproteins H/L bind to cells independently of αVβ3 integrin and inhibit virus entry, and their constitutive expression restricts infection. *J Virol* 84:4013–4025.
32. Galdiero M, et al. (1997) Site-directed and linker insertion mutagenesis of herpes simplex virus type 1 glycoprotein H. *J Virol* 71:2163–2170.
33. Jackson JO, Lin E, Spear PG, Longnecker R (2010) Insertion mutations in herpes simplex virus 1 glycoprotein H reduce cell surface expression, slow the rate of cell fusion, or abrogate functions in cell fusion and viral entry. *J Virol* 84:2038–2046.
34. Wu L, Borza CM, Hutt-Fletcher LM (2005) Mutations of Epstein-Barr virus gH that are differentially able to support fusion with B cells or epithelial cells. *J Virol* 79: 10923–10930.
35. Wu L, Hutt-Fletcher LM (2007) Point mutations in EBV gH that abrogate or differentially affect B cell and epithelial cell fusion. *Virology* 363:148–155.
36. Molesworth SJ, Lake CM, Borza CM, Turk SM, Hutt-Fletcher LM (2000) Epstein-Barr virus gH is essential for penetration of B cells but also plays a role in attachment of virus to epithelial cells. *J Virol* 74:6324–6332.